DOI: 10.1002/cphc.201100759

Direct versus Hydrogen-Assisted CO Dissociation on the Fe(100) Surface: a DFT Study

Mohammad Reza Elahifard, Manuel Pérez Jigato, and J. W. (Hans) Niemantsverdriet*[a]

The Fischer–Tropsch (F-T) synthesis is an important process in modern energy technology, as it enables the conversion of natural gas, coal, or biomass-derived synthesis gas ($CO+H_2$) into hydrocarbon fuels. The process uses iron or cobalt catalysts and depending on the conditions it produces diesel fuel and waxes, or a mixture of smaller hydrocarbons, among which a large fraction consists of olefins and naphtha.[1,2] Many recent computational studies have addressed the mechanism for this reaction.[3–7] Dissociation of the CO bond is a key step in the initiation of the F-T process. In principle it may occur through one of three pathways:[8]

a) $CO_{ads}+*\rightarrow C_{ads}+O_{ads}$
b) $CO_{ads}+H_{ads}\leftrightarrow HCO_{ads}+*\rightarrow HC_{ads}+O_{ads}$
c) $CO_{ads}+Hads\leftrightarrow COH_{ads}+*\rightarrow C_{ads}+OH_{ads}$

where * stands for the active site. The direct reaction (a) has been shown to be energetically feasible on the more reactive surfaces of iron[7,9,10] and on stepped surfaces of cobalt or ruthenium,[8,11] with activation energies in the range of 0.5–1.2 eV. However, on close-packed surfaces, such as Fe(110), Co(0001), and Ru(0001), the activation energies are substantially higher.[12–14] In these cases, the H-assisted routes offer energetically more favourable alternatives.[12,13] H-assisted dissociation has also been found preferred over direct dissociation on carbon-saturated surfaces of the iron carbide Fe_5C_2.[15]

The purpose herein is to compare the energetics of direct and H-assisted CO dissociation on the Fe(100) surface and to compare it to the recently published process on the close-packed (110) surface. This question is relevant because first, the bonding geometry of CO—in a tilted mode—differs from that on the (110) surface, where CO binds perpendicularly. Secondly, the Fe(100) is more reactive, causing the dissociation products C and O to bind stronger than on (110), hence providing a stronger driving force for the direct dissociation. We show that both direct and H-assisted CO dissociation through the HCO intermediate have feasible energetics to occur on the Fe(100) surface in synthesis gas environments, suggesting that both pathways may compete, depending on the conditions.

The resulting total energies for the most stable adsorption sites after geometry optimization of all species appearing in reactions (a)–(c) are displayed in Figure 1 (HCO, COH, $C+O+H$, $CO+H$, $HC+O$), along with the fully computed activation energies (CI-NEB, see Calculation Methods). Figure 2 shows the optimal geometries for the initial states (IS), final states (FS), and transition states (TS) involved in all three possible dissociation routes.

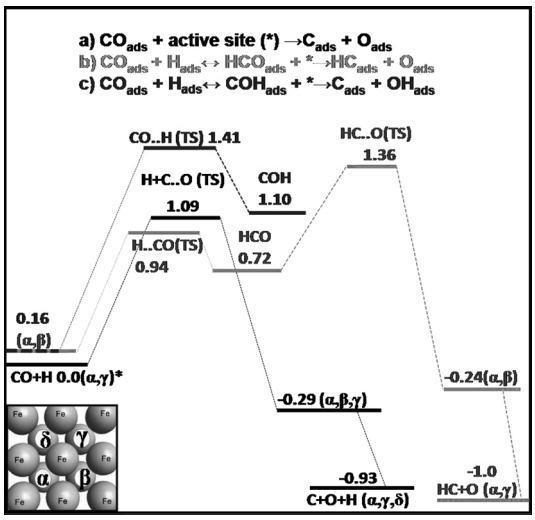

Figure 1. Relative energy of states [eV] and CO dissociation pathways. a) Direct CO dissociation. b) Via HCO intermediate formation. c) Via COH intermediate formation.* The inset clarifies the nomenclature for the hollow sites available for co-adsorption. Symbols in parentheses reference the four-fold hollow site occupied by atoms or a CO molecule as shown in the bottom left of the figure.

The most stable co-adsorption configuration for CO and H on a p(2×2) cell corresponds to a tilted CO on the four-fold hollow site, similarly to that observed on the clean surface.[9] In general, we found that H co-adsorption has a small effect on CO. Our result for the CO-only adsorption energy is 1.5 eV. For CO in the co-adsorption system in the $\alpha\beta$, $\alpha\delta$, and $\alpha\gamma$ configurations the adsorption energies are 1.45, 1.48 and 1.61 eV, respectively.

The direct CO dissociation process is exothermic, with a reaction energy of -0.29 eV. Its final state is determined by the ejected carbon occupying the second nearby hollow-site and subsequently diffusing to the furthest one. The computed C diffusion barrier of ca. 0.7 eV is larger than that of the independent O and H atoms, due to the strong bond between C and the Fe(100) surface[16]. The overall energy balance is -0.93 eV in agreement with previous work.[7,9]

The activation energy for the direct process is 1.09 eV, which is smaller than the CO dissociation barrier when no hydrogen is present (1.2 eV), showing that the H-atom affects the TS more than the IS. On the other hand, Scheijen et al.[7] have found an increase of 0.05 eV in the barrier for CO dissociation when its coverage increased from 0.25 to 0.5 on Fe(100).

[a] M. R. Elahifard, Dr. M. P. Jigato, Prof. Dr. J. W. Niemantsverdriet
Schuit Institute of Catalysis, Eindhoven University of Technology
5600 MB Eindhoven (The Netherlands)
Fax:(+31) 402473481
E-mail: J.W.Niemantsverdriet@tue.nl

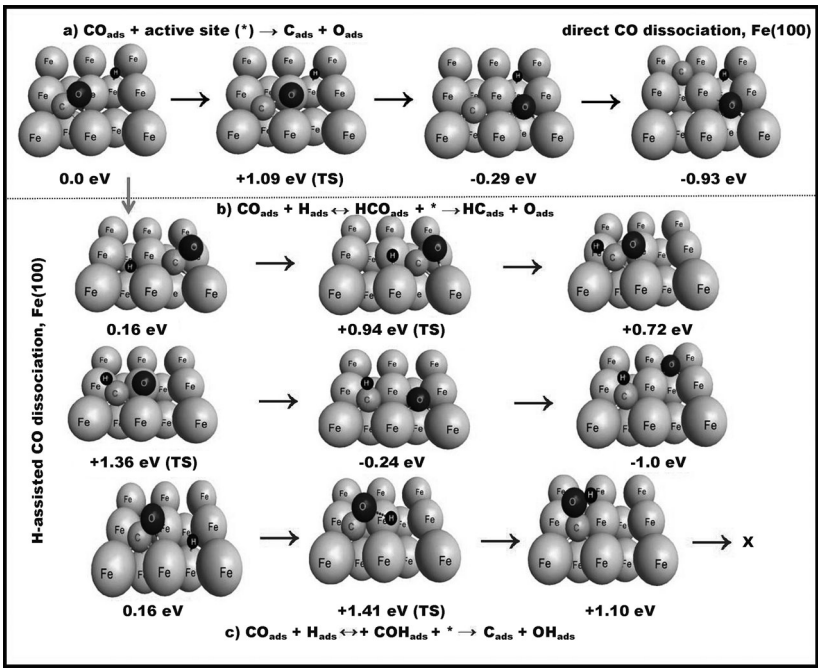

Figure 2. Adsorbate structures for direct and H-assisted CO dissociation on Fe(100) surfaces.

Therefore, the effect of pressure on the activation energies is small on Fe(100). This is in contrast to the results reported by Ojeda et al.[13] on the close-packed Fe(110) surface, where the CO dissociation barrier increased by 0.45 eV as the CO coverage went from 0.25 to 0.5 (in the presence of hydrogen). They reported a high value for the activation energy (1.95 eV) as well as a positive reaction energy of 0.23 eV in the case of direct CO dissociation, showing that in the presence of hydrogen Fe(110) is a clearcut situation with no direct CO dissociation at 50% coverage. The case of Fe(100) is different, because of the moderate energetic barrier and a negative reaction energy for direct CO dissociation. Hence, we conclude that under F-T process conditions (250 °C) CO dissociates considerably through the direct route on Fe(100).

Regarding the H-assisted routes, the formations of HCO and COH are endothermic processes, with reaction energies of +0.56 eV and +0.94 eV. In both cases, the formation of the intermediate is followed by a subsequent dissociation step that leads to the formation of either CH or OH [reactions (b) and (c)].

The energy barrier for HCO formation is 0.78 eV, which is close to the corresponding reaction energy of the first stage of the process (+0.56 eV). Therefore, we conclude that the HCO intermediate on Fe(100) acts as a pre-equilibrium state. The second stage of this process (HCO→HC+O) has an activation energy of 0.64 eV, which is much smaller than the direct CO dissociation barrier and in agreement with previous cluster calculations done for CO on Fe(100).[17]

A barrier of 0.22 eV characterizes the transition state for the reverse process, that is HCO→CO+H. This reaction, compared to the dissociation of HCO into HC+O, would have a rate constant 10^4 times higher at 250 °C (according to the Arrhenius equation). When comparing direct CO dissociation to H-assisted CO dissociation via HCO both effects need to be considered: 1) the barrier for HCO formation is lower than the barrier for direct CO dissociation and 2) the barrier for HCO dissociation into CO+H is much lower compared to the barrier for HCO dissociation into CH+O. The second effect considerably decreases the efficiency of the mechanism via HCO compared to the direct CO dissociation process.

However, under high H_2 pressure and lower temperatures (favouring a low number of unoccupied active sites and a considerable amount of H on the surface), the H-assisted CO dissociation route via HCO is likely to occur. It has to be noted that HCO formation [first stage on path (b)] creates an empty site, while direct CO dissociation consumes an active site. Furthermore, the rate constant difference between direct CO dissociation and the via-HCO H-assisted process increases exponentially upon lowering the temperature. The consequence of having too few active sites is that while the direct route is stopped by site blocking, path (b) suffers a dramatic decrease in conversion efficiency. Therefore, the dominant mechanism for CO dissociation on Fe(100) is proposed to change depending on the conditions.

In principle H-assisted CO dissociation on Fe(100) could also proceed through hydrogenation of the oxygen-end of the CO molecule and forming COH as an intermediate, dissociating further into OH and C. The optimal geometries for both IS and FS for COH formation [first stage on path (c)] display an important difference. While the IS is characterized by a tilted CO molecule, the FS has an upright CO bond as part of the COH intermediate. Furthermore, the CO part of the TS is very similar to that in the IS in the tilted case. The stable upright C–O bond in the FS is therefore only achievable through a significant bending of the OH bond as H approaches CO further at the TS (for a close-packed surface the thermodynamics of the FS would be different, since an IS with upright CO would be favoured). Overall, CO dissociation via the COH intermediate is energetically highly unfavourable.

Finally, the formation processes of HC and OH, subsequent to direct CO dissociation, were investigated for their relevance to hydrocarbon and water formation. From their activation energies (Figure 1), CH formation is more favourable than OH formation (0.74 eV vs. 1.3 eV). Furthermore, CH can form from HCO via dissociation with an energy barrier of 0.64 eV. Figure 3 illustrates the energies for the ISs and FSs, as well as the corresponding TSs (C+O+H→CH+O and C+O+H→C+OH). Regarding OH formation, we conclude that the tilted OH configuration on the bridge site is marginally more stable than the up-

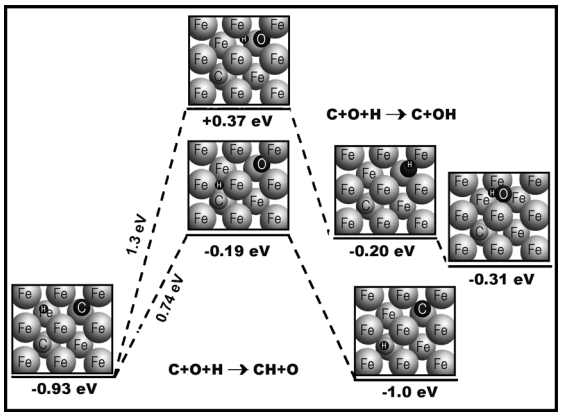

Figure 3. HC and OH formation after direct CO dissociation.

right OH configuration on the hollow site, and that the activation energy to form the tilted configuration on the bridge site is 0.6 eV higher. Therefore, OH forms on the hollow sites (upright) to possibly diffuse to the bridge site (tilted) later on.

In conclusion, we present evidence for the first step in the F-T synthesis (CO dissociation) occurring via both direct (major route) and via-HCO H-assisted (minor route) mechanisms on Fe(100). Under conditions favouring the existence of very few empty sites, only the latter mechanism is expected to contribute, albeit with low efficiency. On an empty surface direct CO dissociation is the preferred pathway on Fe(100), in contrast to Fe(110). Regarding the COH formation route, our results show that this reaction will not take place on Fe(100). Furthermore, after direct CO dissociation, the activation energy for CH formation is half the OH formation barrier.

Calculation Methods

Total energy calculations were carried out with the projector augmented wave (PAW) method as implemented in the Vienna ab initio simulation package (VASP).[18–21] Spin-density-functional theory in the revised form of the Perdew–Burke–Ernzerhof exchange-correlation functional (RPBE) was employed throughout as the correct form of the generalized gradient approximation (GGA) for producing adsorption energies.[22,23] The cutoff energy for the plane wave expansion of the wave functions was 480 eV, and the k-point sampling, generated from the Monkhorst–Pack procedure,[24] used a surface mesh of $5\times5\times1$ and a mesh for body centred cubic (bcc) bulk-Fe of $15\times15\times15$. The Fe(100) surface was modelled with a five layer slab and 12 Å vacuum size, within the three-dimensional supercell, and a p(2×2) unit cell was used to represent the 0.25 ML CO and the 0.25 ML H coverages. The top three layers were relaxed during geometry optimization, stopping when the forces became smaller than 0.01 eV $Å^{-1}$. Our equilibrium lattice constant for bcc Fe was 2.872 Å (RPBE), which agreed with the experimental value of 2.87 Å.[10] The climbing-image nudged elastic band method[25] was applied for transition state search. CI-NEB is a minimum-energy path and transition-state search algorithm that uses both limiting geometries involved in the activated process, that is the IS and the FS. A series of intermediate configurations between those two was built up, and a simultaneous optimisation for all of them was carried out after a spring was set up between all configurations. The highest energy configuration was finally allowed to achieve the saddle point/local maximum through further refinement.

Acknowledgements

This work was sponsored by the National Computing Facilities Foundation NCF (Grant SH-034-11) for the use of supercomputer facilities, with financial support from the Netherlands Organization for Scientific Research (Grant ECHO 700.59.041).

Keywords: CO dissociation · density functional calculations · Fischer–Tropsch mechanism · iron · surface chemistry

[1] H. Storch, N. Golumbic, R. B. Anderson, *The Fischer–Tropsch and Related Synthesis* Wiley, New York, **1951**.
[2] B. H. Davis, *Catal. Today* **2003**, *84*, 83–98.
[3] D. Curulla-Ferré, A. Govender, T. C. Bromfield, J. W. Niemantsverdriet, *J. Phys. Chem. B* **2006**, *110*, 13897–13904.
[4] D. E. Jiang, E. A. Carter, *J. Phys. Chem. B* **2006**, *110*, 22213–22219.
[5] D. C. Sorescu, *Phys. Rev. B* **2006**, *73*, 155420–155436.
[6] M. Ojeda, A. Li, R. Nabar, A. U. Nilekar, M. Mavrikakis, E. Iglesia, *J. Phys. Chem. C* **2010**, *114*, 19761–19770.
[7] F. J. E. Scheijen, D. Curulla-Ferré, J. W. Niemantsverdriet, *J. Phys. Chem. C* **2009**, *113*, 11041–11049.
[8] S. Shetty, A. P. J. Jansen, R. A. van Santen, *J. Am. Chem. Soc.* **2009**, *131*, 12874–12875.
[9] T. C. Bromfield, D. Curulla-Ferré, J. W. Niemantsverdriet, *ChemPhysChem* **2005**, *6*, 254–260.
[10] D. C. Sorescu, *J. Phys. Chem. C* **2008**, *112*, 10472–10489.
[11] S. Shetty, R. A. van Santen, *Phys. Chem. Chem. Phys.* **2010**, *12*, 6330–6332.
[12] O. R. Inderwildi, S. J. Jenkins, D. A. King, *J. Phys. Chem. C* **2008**, *112*, 1305–1307.
[13] M. Ojeda, R. Nabar, A. U. Nilekar, A. Ishikawa, M. Mavrikakis, E. Iglesia, *J. Catal.* **2010**, *272*, 287–297.
[14] D. E. Jiang, E. A. Carter, *Surf. Sci.* **2004**, *570*, 167–177.
[15] J. M. Gracia Budria, F. F. Prinsloo, J. W. Niemantsverdriet, *Catal. Lett.* **2009**, *133*, 257–261.
[16] D. E. Jiang, E. A. Carter, *Phys. Rev. B* **2005**, *71*, 45402–45407.
[17] G. Blyholder, M. Lawless, *Langmuir* **1991**, *7*, 140–141.
[18] G. Kresse, J. Furthmüller, *Comput. Mater. Sci.* **1996**, *6*, 15–50.
[19] G. Kresse, J. Hafner, *Phys. Rev. B* **1994**, *49*, 14251–14269.
[20] P. E. Blöchl, *Phys. Rev. B* **1994**, *50*, 17953–17979.
[21] G. Kresse, D. Joubert, *Phys. Rev. B* **1999**, *59*, 1758–1775.
[22] J. P. Perdew, K. Burke, M. Ernzerhof, *Phys. Rev. Lett.* **1996**, *77*, 3865–3867.
[23] B. Hammer, *Phys. Rev. B* **1999**, *59*, 7413–7421.
[24] H. J. Monkhorst, J. D. Pack, *Phys. Rev. B* **1976**, *13*, 5188–5192.
[25] G. Henkelman, B. P. Uberuaga, H. Jónsson, *J. Chem. Phys.* **2000**, *113*, 9901–9904.

Received: September 28, 2011
Revised: October 25, 2011
Published online on December 6, 2011

